

## Failure of chaos control

Willem van de Water and John de Weger

*Physics Department, Eindhoven University of Technology, P.O. Box 513, 5600 MB, Eindhoven, The Netherlands*

(Received 4 May 2000)

We study the control of chaos in an experiment on a parametrically excited pendulum whose excitation mechanism is not perfect. This imperfection leads to a weakly excited degree of freedom with an associated small eigenvalue. Although the state of the pendulum could be characterized well and although the perturbation is weak, we fail to control chaos. From a numerical model we learn that the small eigenvalue cannot be ignored when attempting control. However, the estimate of this eigenvalue from an (experimental) time series is elusive. The reason is that points in an experimental time series are distributed according to the natural measure. It is this extremely uneven distribution of points that thwarts attempts to measure eigenvalues that are very different. Another consequence of the phase-space distribution of points for control is the occurrence of logarithmic-oscillations in the waiting time before control can be attempted. We come to the conclusion that chaos needs to be destroyed before the information needed for its control can be obtained.

PACS number(s): 05.45.-a

### I. INTRODUCTION

In the past few years the control of chaos has evolved into a very actively pursued application of nonlinear dynamics. Chaos is full of unstable periodic orbits which visit phase space in a huge variety of ways and which have periods of almost any length. When given enough time, a chaotic trajectory will pass arbitrarily close to each of them. The key idea by Ott, Grebogi, and Yorke [1] is that it can be steered onto the unstable periodic point when it is close enough using modulation of a system parameter. The magnitude of these modulations must be sufficient to capture the system into a periodic orbit when it is near, but can decrease to almost zero when the system is exactly on the orbit.

A central notion is that all needed information can be learned from an experimental time series of measurements on the chaotic system. It is not even necessary to perform a complete measurement of the system's phase space, as embedding techniques [2] can be used to reconstruct the phase space from a measurement of a single (scalar) component. This information can be used to trace the location of unstable periodic orbits, and to deduce the dynamics of their local linear neighborhoods. Thus, chaotic dynamics of any low-dimensional system can be turned into the regular motion of choice without detailed knowledge of the dynamical system and using parameter modulations that are just large enough to overcome the intrinsic noise of the system and the measurement. This exciting idea motivated the present work.

We have tried to control chaos in an experiment of a parametrically excited pendulum, but failed. On the other hand, there are numerous reports of successful chaos control [4–7]. Our failure was also surprising because we were able to precisely characterize the chaotic state and found very favorable agreement with a faithful numerical simulation [3]. The failure of this experiment made us consider carefully the ideas of controlling chaos.

Analysis of the experiment revealed that an extra mode of motion exists that is related to a weak interaction of the pendulum with its driving. As the associated eigenvalue is small, this mode is stiff and adjusts quickly to the state of the pendulum. In a numerical model we quantify this interaction

through a dynamical invariant. The strength of the interaction and, therefore, the importance of the parasitic mode are set by a single parameter in our numerical simulation. For most parameter settings, dynamical invariants of the system are not affected by this mode. It is, therefore, dynamically irrelevant most of the time. Still, it has a dramatic influence on the possibility of controlling the system. Thus, to design the control strategy, the associated small eigenvalue must be known.

If no other information is available in an experiment, the linear neighborhood of an unstable periodic point must be learned from an experimental time series. The points that happen to be close to the unstable periodic point can be used in a least-squares analysis to determine the local linear dynamics near the unstable periodic point. In our case, the associated matrix has both large and small eigenvalues. In any registered time series the points are distributed according to the natural measure. It was already noted in [8,9] that this hinders an accurate estimate of the eigenvalues. In the present paper we quantify this error amplification by introducing a condition number which exhibits interesting scaling behavior. For the perturbed pendulum this number is so large that it becomes impossible to learn the needed information from a time series, even in the absence of noise.

Control of chaos separates into two distinct problems. The first one is how to modulate the system parameter, given the linear environment of the unstable periodic point whose stabilization is sought. This problem is entirely within the realm of control theory, and a plethora of techniques exists to solve it [10]. A perhaps more interesting aspect is related to the structure of phase space of chaotic nonlinear systems: the question here is which unstable periodic points exist, and how long one has to wait before a chaotic orbit comes close enough to a periodic point and control can become effective. As we found, a third question is how chaos affects the estimate of the dynamics in small neighborhoods of unstable periodic points. In our experiment the necessity for considering small eigenvalues for control is rooted in control engineering, but the impossibility of measuring them is related to the structure of phase space.

In Sec. II we will describe the experiment and formulate a

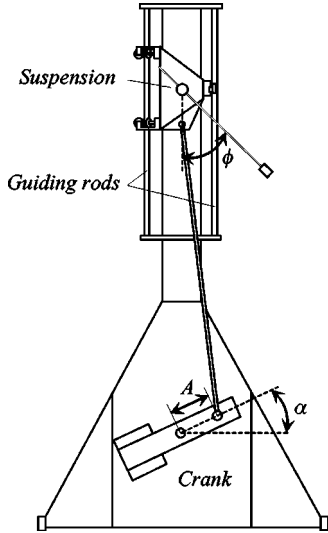


FIG. 1. The parametric pendulum, drawn to scale; its height is 1.38 m. A bob with an effective mass of  $m=0.0858$  kg is attached to a rod of  $l=0.317$  m length and negligible mass. The angle  $\phi$  is read with help of a 12 bit optical encoder. The suspension has a mass  $m_s$  of 0.5 kg. It is driven with a driving rod with length  $l_c=0.75$  m and a crank with arm  $A=0.13$  m and moment of inertia  $I_c=0.08$  kg m<sup>2</sup>. The damping constants of the pendulum used in Eq. (1) are  $k_1=0$ ,  $k_2=0.05639$  s<sup>-1</sup>, and  $k_3=0.02209$ . The two angles  $\phi$  and  $\alpha$  are the dynamical variables.

model differential equation for the weak interaction of the pendulum with its drive. Next, we will analyze dynamical invariants as a function of the parameter that controls the strength of the interaction. For most values of this parameter, the mode associated with the perturbation is very weak and the question is if chaos can be achieved while ignoring this mode. In Sec. IV we give the control matrix for this approach, and conclude that such control will not work unless the extra mode is very weak. In Sec. V we discuss the least-squares estimate of this mode and the adverse effect of the structure of the natural measure on the errors of such an estimate. In Sec. VI we analyze the average waiting time before control can become effective as a function of the maximum control action. Both this waiting time and the error amplification reflect the Cantor-like structure of the natural measure. We conclude that chaos must be destroyed before we can learn the information needed for controlling it.

## II. PARAMETRIC PENDULUM

The parametric pendulum is a nonlinear system which features a chaotic state whose basin of attraction occupies a large portion of phase space. It thus is ideally suited to studying control of chaos.

A schematic view of the experiment is shown in Fig. 1. The pendulum is a massless rod of 0.317 m length, ending in a bob with an effective weight of 0.0858 kg. Its angular position  $\phi$  can be read using a 12 bit encoder. A  $\dot{\phi}$  velocity measurement is done by finite difference. The support of the pendulum is oscillated vertically with frequency  $\Omega$  using a crank mechanism. A true Poincaré section is obtained by reading  $\phi$  and  $\dot{\phi}$  when the support of the pendulum is in its highest position.

The  $(\phi, \dot{\phi})$  dynamical state of the pendulum is described by the equation of motion

$$\ddot{\phi} + \frac{k_1}{m l^2} \text{sgn}(\dot{\phi}) + \frac{k_2}{m l^2} \dot{\phi} + \frac{k_3}{m l^2} (\dot{\phi})^2 \text{sgn}(\dot{\phi}) + \left\{ \omega_0^2 - \frac{G(t)}{l} \right\} \sin(\phi) = 0, \quad (1)$$

where  $\omega_0=(g/l)^{1/2}$  is the eigenfrequency of the pendulum. The acceleration of the pendulum suspension  $G(t)$  is proportional to  $\cos(\Omega t)$ , but the crank mechanism used contributes higher harmonics

$$G(t) = A \left\{ \cos(\Omega t) + \epsilon \frac{\cos(2\Omega t) + \epsilon^2 \sin^4(\Omega t)}{[1 - \epsilon^2 \sin(\Omega t)]^{3/2}} \right\} \Omega^2, \quad (2)$$

where  $A$  is the length of the driving arm of the crank mechanism and  $\epsilon$  is the ratio of  $A$  to the length of the other arm. The damping constants  $k_{1-3}$  were determined experimentally. The presence of the Coulomb friction term (proportional to  $k_1$ ) is essential for the asymptotic state of the pendulum. It gives rise to a small island of stability at the origin of the  $(\phi, \dot{\phi})$  phase plane which lies in a sea of chaos. As a consequence, all chaos is transient, although these transients may last several hours. A slight complication of the Coulomb friction is that the pendulum may become stuck near its downward position and may be shaken loose again at a later instant during one excitation cycle. Our numerical procedure adequately handles these complications, but in order to avoid restarting the integration while generating long time series we performed all numerical simulations with the Coulomb friction coefficient set to zero. As our interest is in a faithful numerical simulation of the experiment, we care about these details. They are, however, not relevant for our conclusion.

In our experiments, the vertical oscillatory motion of the support of the pendulum is driven by a crank mechanism using a 1 kW motor with tachogenerator feedback. This feedback mechanism is not perfect and the angular velocity of the crank varies approximately by 5%. Clearly, the feedback mechanism cannot cope perfectly with the varying load exerted by the chaotically swinging pendulum. As mentioned in the Introduction, this imperfection has dramatic consequences for the controllability of unstable periodic orbits. In order to understand this, let us introduce a version of our pendulum model that faithfully mimics the nonidealities of the experiment. We will do that by extending Eq. (1) with a differential equation for the angular velocity feedback.

Let us call the angular velocity of the driving crank  $\dot{\alpha}$ . In the nonideal experiment,  $\dot{\alpha}$  is not a constant, but will vary due to the fluctuating load of the chaotically swinging pendulum. It is in this way that the pendulum interacts with its environment. A simple model for the driving feedback mechanism is

$$I_c \ddot{\alpha} = -M(\phi, \dot{\phi}, \ddot{\phi}, \alpha) + K_p(\Omega - \dot{\alpha}) + K_d \ddot{\alpha}, \quad (3)$$

where  $I_c$  is the moment of inertia of the crank and  $M$  is the torque that is exerted by the pendulum and its suspension on the driving crank, which depends on the dynamical state

$(\phi, \dot{\phi})$ ; it is specified below. In the feedback mechanism  $K_p(\Omega - \dot{\alpha}) + K_d\ddot{\alpha}$ ,  $\Omega$  is the set frequency,  $K_p$  is the proportional feedback constant, and  $K_d$  is the integral feedback constant (which can be trivially absorbed in the moment of inertia  $I_c$  of the crank).

In the limit  $K_p = \infty$  the angular frequency  $\dot{\alpha}$  is constant,  $\dot{\alpha} = \Omega$ , and the pendulum does not interact with its environment. For decreasing  $K_p$  the influence of the driving mechanism on the state  $(\phi, \dot{\phi})$  of the pendulum and vice versa increases and at  $K_p = 0$  the angular frequency of the drive is simply uncontrolled. At finite  $K_p$ , when the driving frequency is no longer a constant, the acceleration  $G(t)$  of the pendulum suspension [Eq. (2)] becomes

$$G(t) = A \left\{ \cos \alpha + \frac{\epsilon \cos 2\alpha + \epsilon^3 \sin^4 \alpha}{(1 - \epsilon^2 \sin^2 \alpha)^{3/2}} \right\} (\dot{\alpha})^2 + A \left\{ \sin \alpha + \frac{\epsilon \sin \alpha \cos \alpha}{(1 - \epsilon^2 \sin^2 \alpha)^{1/2}} \right\} \ddot{\alpha}. \quad (4)$$

Thus, our model turns from a second-order nonautonomous dynamical system into a fourth-order autonomous one.

A simple geometrical argument gives for the moment that the pendulum exerts on its driving

$$M(\phi, \dot{\phi}, \ddot{\phi}, \alpha) = \{mg + (m + m_s)G(t) + ml[(\dot{\phi})^2 \cos \phi + \ddot{\phi} \sin \phi]\} A \sin \alpha, \quad (5)$$

where  $m_s$  is the mass of the suspension (see Fig. 1). We emphasize that the details of our model, such as the precise form of the driving term Eq. (4), are irrelevant for the conclusions reached; what matters is the existence of a parameter  $K_p$  that gauges the nonideality of the parametric pendulum.

For finite values of  $K_p$ , the dynamics of the perturbed pendulum no longer takes place in a two-dimensional stroboscopic plane, but involves the four-dimensional  $(\phi, \dot{\phi}, \alpha, \dot{\alpha})$  space. Assuming that the feedback control is effective enough to prevent sign reversal of  $\dot{\alpha}$ , a three-dimensional Poincaré space  $(\phi, \dot{\phi}, \dot{\alpha})$  results from intersecting the orbit with the plane  $\alpha = \pi$ . Therefore, the interaction of the pendulum with its excitation extends phase space with one extra dimension.

Obviously, as the fluctuations in  $\dot{\alpha}$  are small, the new three-dimensional space is a flat pancake which gets thinner in the  $\dot{\alpha}$  direction with increasing constant of proportional feedback  $K_p$ . Both for the isolated pendulum and for the perturbed case, a mapping  $F$  can be defined that evolves phase-space points between two subsequent Poincaré sections ( $\alpha = \pi$ ),

$$\xi_{n+1} = F(\xi_n). \quad (6)$$

For the unperturbed pendulum this is trivially the same as a stroboscopic map at times  $t_n = n2\pi/\Omega$ . From now on we will study the dynamics of the pendulum through iterations of the map  $F$ . Of course, a computation of  $F$  involves integration of the equations of motion.

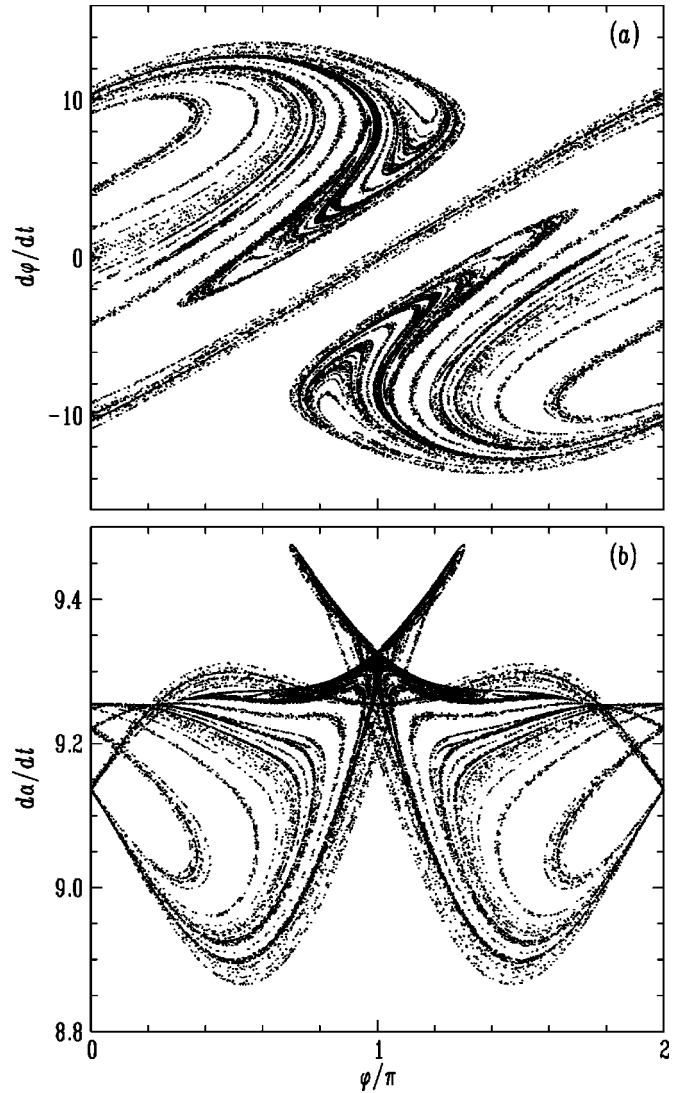


FIG. 2. Chaotic attractor of perturbed pendulum driven at a set  $\Omega = 9.09 \text{ s}^{-1}$ , and with a coupling feedback constant  $K_p = 0.59 \text{ kg m}^2 \text{ s}^{-1}$ . (a) View of the  $(\phi, \dot{\phi})$  section of the three-dimensional Poincaré space. (b) View of the  $(\phi, \dot{\alpha})$  section of the Poincaré space. The angular velocities  $\dot{\phi}$  and  $\dot{\alpha}$  are in  $\text{s}^{-1}$ . The finite value of the feedback constant causes chaotic fluctuations of the angular velocity  $\dot{\alpha}$  of the driving.

The linear neighborhood of a point  $\xi_0$  evolves under the action of the Jacobian  $\mathbf{A}$  of the map,  $A_{ij} = \partial F_i / \partial \xi_j |_{\xi = \xi_0}$ . In a fixed point, the Jacobian has real eigenvalues with the smallest one  $\lambda_3$  determined by the nonideality of the driving. For large  $K_p$  the reaction  $M$  on the driving mechanism of the pendulum in Eq. (3) can be ignored, and

$$\lambda_3 \approx \exp \left\{ -\frac{2\pi K_p}{\Omega(I_c - K_d)} \right\}. \quad (7)$$

If the constant of the proportional driving feedback tends to infinity, the driving angular velocity is a constant and  $\lambda_3$  tends to zero. When the driving feedback constant vanishes, the restoring force disappears, and  $\lambda_3$  tends to 1.

The  $(\phi, \dot{\phi})$  projection of the chaotic attractor at  $K_p = 0.59$  is shown in Fig. 2(a). It is very similar to the phase

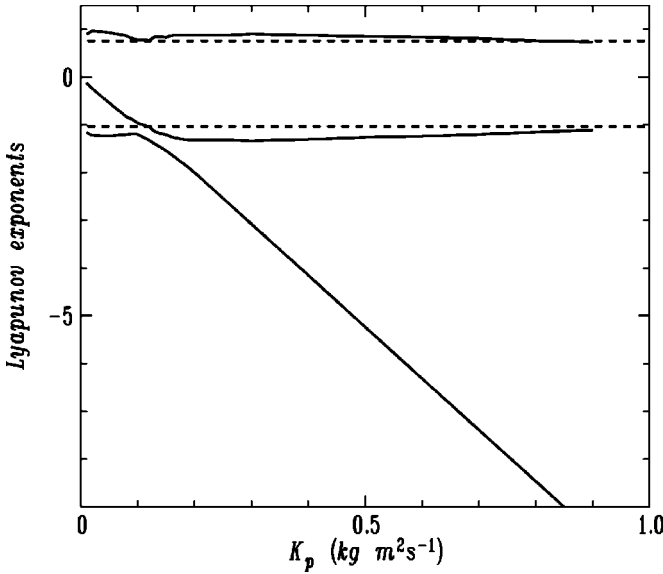


FIG. 3. Full lines: Lyapunov exponents of a pendulum that interacts with its driving. Dashed lines: Lyapunov exponents of the isolated pendulum (which has a two-dimensional phase space).

plane of the unperturbed pendulum [3]. The difference is that the interaction of the pendulum with its excitation results in dynamical behavior of the excitation angular velocity  $\dot{\alpha}$ . The  $(\phi, \dot{\alpha})$  projection of the Poincaré space is shown in Fig. 2(b). At this value of the feedback parameter, the chaotic fluctuation of  $\dot{\alpha}$  is about 6%, which is comparable to that observed experimentally. A fundamental question is, however, whether the  $\dot{\alpha}$  dynamics constitutes an essential new degree of freedom of the perturbed pendulum, or whether it is merely slaved to that of the  $(\phi, \dot{\phi})$  pendulum state. To answer this question, we will study the evolution of a dynamic invariant with the strength of the perturbation.

As dynamical invariants we computed the three Lyapunov exponents that gauge the average sensitivity to variation of initial conditions along a chaotic orbit from the map Eq. (6). The Lyapunov exponents of the perturbed pendulum are shown in Fig. 3. For large feedback parameter  $K_p$  Eq. (7) predicts that  $\lambda_3$  goes to  $-\infty$  as  $-2\pi K_p / \Omega(I_c - K_d)$ . In this case the largest and next-largest Lyapunov exponents  $\lambda_{1,2}$  approach those of the isolated pendulum. We believe that the ‘‘anticrossing’’ behavior of the Lyapunov exponents at  $K_p \approx 0.15$  is the consequence of the well-known Wigner–von Neumann ‘‘no crossing rule,’’ which states that the eigenvalues of a real symmetric matrix generically do not cross if a parameter is varied.

From the spectrum of Lyapunov exponents it is possible to derive the fractal dimension of the chaotic attractor. The argument is that the integer part of the dimension is given by the number  $K$  of expanding directions in phase space along which the measure is smooth, with  $K$  given by  $\sum_{i=1}^K \lambda_i \geq 0$ . The fractional part of the dimension is the ratio of contraction and expansion [11]

$$D_L = K + \frac{1}{|\lambda_{K+1}|} \sum_{j=1}^K \lambda_j. \quad (8)$$

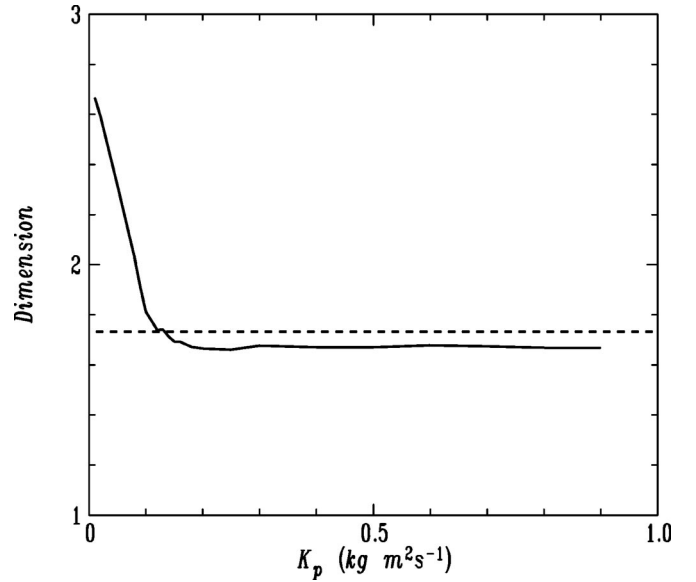


FIG. 4. Full line: Lyapunov dimension of a pendulum that interacts with its driving as a function of the driving feedback parameter  $K_p$ . Dashed line: Lyapunov dimension of the isolated pendulum.

The Lyapunov dimension as a function of  $K_p$  is shown in Fig. 4. It is a striking observation that the attractor dimension has already reached its asymptotic value at  $K_p \approx 0.2$ . From then on, the relevant embedding space is two-dimensional and the dynamics of the  $\dot{\alpha}$  degree of freedom apparently no longer has a life of its own and must be merely slaved to the dynamics of the  $(\phi, \dot{\phi})$  subspace. Information about it might no longer be needed when controlling chaos. As the  $\dot{\alpha}$  degree of freedom adjusts rapidly to the  $(\phi, \dot{\phi})$  state, it might be removed altogether by adiabatic elimination. However, we do not know how to do this by using information from an experimental time series only.

### III. CONTROLLING UNSTABLE PERIODIC ORBITS

If no *a priori* information is available about the experimental system, unstable periodic points must be found from a registered chaotic time series. For controlling one of those, it is also necessary to learn the linearized dynamics  $\mathbf{A}$  in a small neighborhood of it. Finding unstable periodic points amounts to finding close returns in the time series. A phase-space point  $\xi_k$  that almost returns in  $p$  steps,  $\xi_{k+p} \approx \xi_k$ , is probably close to a true  $p$ -periodic point, especially if a whole neighborhood of  $\xi_k$  returns in  $p$  steps. The linear evolution of points  $\xi_i$  in a small neighborhood of  $\xi_k$  is determined by the Jacobian  $\mathbf{A}$  as  $\xi_{i+p} - \xi_{k+p} = \mathbf{A}(\xi_i - \xi_k)$ , where  $\xi_{i+p}$  is the image of  $\xi_i$  in the rapidly expanding neighborhood of  $\xi_{k+p}$ . The elements of the matrix  $\mathbf{A}$  can be found from a least-squares procedure. The matrix  $\mathbf{A}$  can be used to approximate the true location of the  $p$ -periodic point  $\phi_p$

$$\phi_p = \xi_k + (\mathbf{I} - \mathbf{A})^{-1}(\xi_{k+p} - \xi_k),$$

where  $\mathbf{I}$  is the unit matrix. In our procedure we take the points used for a least-squares estimate of  $\mathbf{A}$  from a ball with radius  $r$  around the nearly returning point  $\xi_k$ . In an experi-

ment, points within a noise radius  $r_i < r$  can be excluded, so that the ball turns into an annulus. The radius  $r$  must be small enough so that the evolution of the balls' contents can still be considered linear.

A successful quest for close returns needs a long time series, especially if close returns near unstable periodic points with large eigenvalues are sought. To search for such close returns, we used the efficient procedures described by Theiler [12].

So far, we have just assumed that the least-squares procedure to find the dynamics in the linear neighborhood of the unstable periodic point always works. As will be explained in Sec. V there are serious problems with this procedure. Remarkably, these problems are caused by the *nonlinearity* of the dynamics that distributes points over phase space. Let us first describe the technique to control unstable periodic motion, and worry about ways to obtain the needed information later on.

In the method sketched by Ot, Grebogi, and Yorke, [1] controlling unstable periodic orbits  $\phi$  can be done if their location depends on a parameter  $q$  (for which we will use the excitation frequency  $\Omega$ ),  $\phi^q = \phi + qg$ . Setting  $q$  to  $q_n$  at each iteration alters the dynamics in a linear neighborhood of the unstable periodic point to

$$\xi_{n+1} = \mathbf{A}\xi_n + q_n \mathbf{u}, \quad (9)$$

with  $\mathbf{u} = (\mathbf{I} - \mathbf{A})\mathbf{g}$ , and where from now on we will place the unstable periodic point at the origin. The quest of the controller is for a vector  $\mathbf{K}$  such that parameter variations  $q_n = \mathbf{K} \cdot \xi_n$  lead to successful control. From Eq. (9) it then follows that

$$\xi_{n+1} = (\mathbf{A} + \mathbf{u} \otimes \mathbf{K}) \xi_n \equiv \mathbf{C} \xi_n, \quad (10)$$

which defines the control matrix  $\mathbf{C}$ . For successful control, the largest eigenvalue of the control matrix must have modulus less than 1.

A geometrically appealing solution to the control problem was given in [1] by choosing

$$\mathbf{K} = -\mathbf{f}_u \cdot \mathbf{A} / (\mathbf{f}_u \cdot \mathbf{u}) \quad (11)$$

where the contravariant vector  $\mathbf{f}_u$  has unit length and is perpendicular to all stable eigenvectors  $\mathbf{e}_{s_i}$ . The strategy of Eq. (11) is to steer the orbit onto the space spanned by the stable eigenvectors of  $\mathbf{A}$ . The choice Eq. (11) is equivalent to

$$q_n = \frac{\lambda_u (\mathbf{f}_u \cdot \xi_n)}{(\lambda_u - 1) (\mathbf{f}_u \cdot \mathbf{g})}, \quad (12)$$

where  $\lambda_u$  is the single unstable eigenvector of  $\mathbf{A}$ . Consequently, the control matrix  $\mathbf{C}$  has eigenvalues  $\lambda_{s_i}$  with accompanying eigenvectors  $\mathbf{e}_{s_i}$  and eigenvalue 0 with right and left eigenvectors  $\mathbf{f}_u$  and  $\mathbf{e}_u - \mathbf{u} / (\mathbf{f}_u \cdot \mathbf{u})$ , respectively. Therefore, the choice Eq. (11) for the control vector  $\mathbf{K}$  completely eliminates the unstable direction of  $\mathbf{A}$ .

This control scheme can be extended naturally to the control of unstable cycles with a longer periodicity. The idea is to execute a control action upon each Poincaré section, and not to wait until the full cycle is completed. The technique is explained in Appendix A, with a resulting control recipe

which is very similar to Eq. (11). Similarly, this approach can be used to enact control at multiple sections  $\alpha_i = 2\pi/N, i = 1, \dots, N$ .

The discrete control action of Eq. (11) assumes that the very change of the parameter  $q$  does not induce a dynamics of its own. For the parametric pendulum it is not possible to suddenly change the excitation frequency as it implies an infinite acceleration of the pendulum support. In practice, the excitation will not be able to cope with such a change and the true excitation frequency will lag. This is actually accounted for in our model, where the parameter  $q (= \Omega)$  is the set point of the driving frequency. It is possible to change this set point suddenly.

For the control scheme to work, a trivial requirement is that the unstable periodic point moves when the control parameter is varied. Thus, by symmetry, the unstable point of the upright pendulum cannot be controlled in this manner. The upright pendulum can, however, be stabilized by choosing an appropriate excitation frequency  $\Omega$ . Acheson and Mullin [13] show that this principle actually extends to multiple coupled upright pendulums.

An interesting question is how long one has to wait before a chaotically wandering orbit is near enough to an unstable periodic point and control can become effective. The displacement of the unstable periodic point in the direction perpendicular to  $\mathbf{e}_s$  is proportional to  $q_n$ . If there exists a maximal allowed parameter modulation  $q_{\max}$ , which is, for example, given by the requirement that the system may not be perturbed too strongly, control can only take effect when a chaotic iterate falls in a strip  $S$  of width  $l_u$  along the stable eigenvector  $\mathbf{e}_s$ . The control scheme of Eq. (11) is based on a linear approximation of the local dynamics. Nonlinearity will be felt if the phase-space point is too far away from the unstable periodic point. Therefore, the length  $l_s$  of the region  $S$  of effective control is limited by the curvature of the stable manifold. As nonlinearities will start quadratically,  $l_s \sim l_u^{1/2}$ . If nothing is done to steer the chaotic orbit toward the strip  $S$ , the waiting time before control can take effect for an arbitrary initial condition is inversely proportional to the measure of  $S$ . It can be shown simply [1] that the measure of  $S$  scales with  $q_{\max}$  as

$$\mu_S \sim (q_{\max})^{1 - (\ln|\lambda_u| / \ln|\lambda_s|) / 2}. \quad (13)$$

Accordingly, the waiting time  $T_w$  before control can be enacted scales with the maximum allowed parameter modulation as  $T_w \sim \mu_S^{-1}$ .

Soon after [1], it was emphasized [14] that the quest for a control vector  $\mathbf{K}$  for a given matrix  $\mathbf{A}$  and displacement vector  $\mathbf{u}$  is a central problem of control theory. There exists a wide variety of solutions to this problem that lead to successful control. Under certain conditions, a vector  $\mathbf{K}$  can be found for any choice of the desired eigenvalues of the control matrix  $\mathbf{C}$  [10]. In control engineering, finding the control vector  $\mathbf{K}$  is called ‘‘pole placement.’’

The choice of Eq. (11) is one of many possibilities, but it is special because it maximizes the area  $S$  of successful control and thus minimizes the waiting time before control can become effective [14]. The intuitively appealing interpretation of Eq. (11) may lead to the erroneous impression that in systems with more than one unstable eigenvector variation of

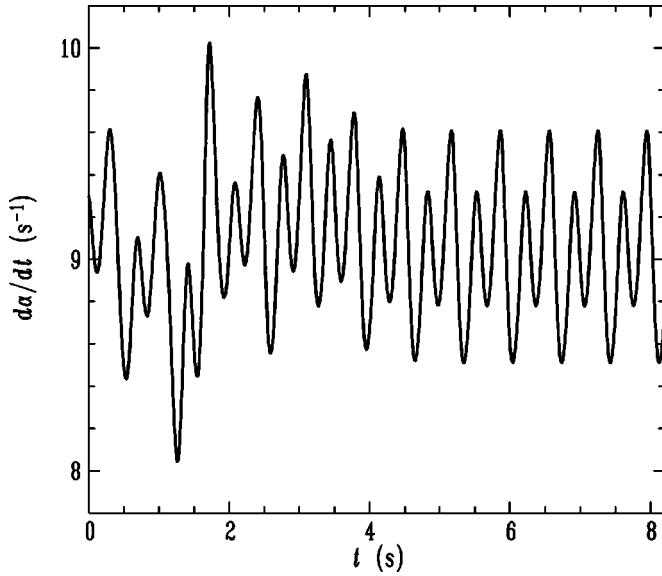


FIG. 5. The angular velocity  $\dot{\alpha}$  of the pendulum driven at  $\Omega = 9.09 \text{ s}^{-1}$  at driving feedback parameter  $K_p = 0.59 \text{ kg m}^2 \text{ s}^{-1}$  while it is captured in an unstable fixed point.

a single system parameter generically cannot lead to successful control. This is clearly contradicted by the cited elementary result of control theory [10] and by experiments [7]. On the other hand, the general pole-placement recipe of control theory is blind to the local structure of phase space. Pole placement allows the specification of eigenvalues of  $\mathbf{C}$ , but not its *eigenvectors*.

#### IV. USING PARTIAL INFORMATION

If complete state information is known, such as the location of the unstable periodic points and their stable and unstable eigenvalues and eigenvectors, the control method sketched in Sec. III will also work for the perturbed pendulum. This is demonstrated in Fig. 5 where at  $K_p = 0.59$  the angular velocity  $\dot{\alpha}$  of the pendulum is shown while it is captured in a fixed point. In this case the periodic point  $\phi_1$  and its eigenvectors were found numerically from Eqs. (1) and (3)–(5). As seeds for the Newton procedure used to find  $\phi_p$  we have used close returns from a long time series [15].

Not only is the mode of motion associated with the variation of  $\dot{\alpha}$  dynamically irrelevant for most  $K$ -values, but we will also show that information about it is extremely hard to come by from an experimental time series. The question then is whether control can be achieved by simply ignoring this mode of motion. Thus, we will try control that is based on *reduced* state space information where only the dynamics in the  $(\phi, \dot{\phi})$  plane is considered and no use is made of the  $\dot{\alpha}$  mode. Of course, the answer is affirmative in the case of large values of the feedback parameter  $K_p$ , when the interaction between the pendulum and its excitation vanishes and the state of the pendulum is completely determined by the coordinates in the  $(\phi, \dot{\phi})$  phase plane alone.

A quantitative answer can be given by considering the reduced control matrix  $\tilde{\mathbf{C}}$  which is defined as

$$\tilde{\mathbf{C}} = \mathbf{A} + \mathbf{u} \otimes \tilde{\mathbf{K}}, \quad (14)$$

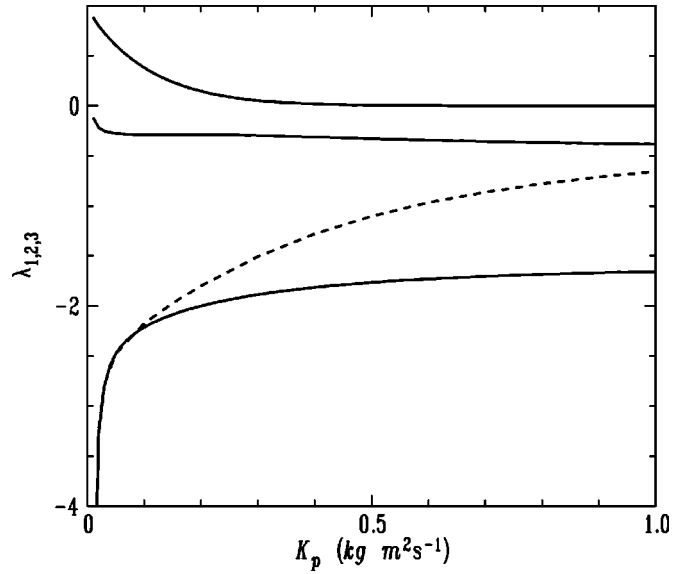


FIG. 6. Controllability of an unstable fixed point in the perturbed pendulum as a function of the driving feedback parameter  $K_p$  using reduced information. Full lines: eigenvalues of the fixed point; dashed line: largest eigenvalue  $\lambda_c$  of the control matrix  $\tilde{\mathbf{C}}$ . For values  $K_p > 0.59 \text{ kg m}^2 \text{ s}^{-1}$ ,  $|\lambda_c| < 1$  and control based on reduced phase-space information is successful.

with a reduced control vector  $\tilde{\mathbf{K}}$  which is constructed out of two-dimensional  $(\phi, \dot{\phi})$  information only with no use made of the  $\dot{\alpha}$  degree of freedom. In analogy with Eq. (11),

$$\tilde{\mathbf{K}} = -\tilde{\mathbf{f}}_u \cdot \tilde{\mathbf{A}} / (\tilde{\mathbf{f}}_u \cdot \tilde{\mathbf{u}}), \quad (15)$$

where the matrix  $\tilde{\mathbf{A}}$  is formed by writing zeros in the third row and the third column of  $\mathbf{A}$ , with  $\tilde{\mathbf{f}}_u$  the contravariant unstable eigenvector and  $\tilde{\mathbf{u}} = (\mathbf{I} - \tilde{\mathbf{A}})\tilde{\mathbf{g}}$ , with  $\tilde{\mathbf{g}}$  the projection of the displacement vector  $\mathbf{g}$  on the  $(\phi, \dot{\phi})$  phase plane.

The result of this information reduction for stabilization of a fixed point is shown in Fig. 6 where the largest eigenvalue  $\lambda_c$  of the control matrix is shown together with the eigenvalues of the unstable fixed point whose stabilization is attempted. In the case of the unperturbed pendulum (at  $K_p = \infty$ ),  $\lambda_c$  approaches the second eigenvalue  $\lambda_{s_2}$  of  $\mathbf{A}$  in agreement with the eigenvalue of the control matrix for control with full state information. For decreasing  $K_p$ ,  $|\lambda_c|$  increases, and at  $K_p < 0.59$  two-dimensional control fails. This is a surprisingly large value because at this point the dynamics of the perturbed pendulum is essentially two dimensional according to Fig. 4. Apparently, for control to be effective we are forced to consider the irrelevant dynamics of the  $\dot{\alpha}$  degree of freedom. When  $K_p$  is decreased further and the perturbation of the pendulum becomes more important,  $\lambda_c$  tends to the largest eigenvalue of  $\mathbf{A}$ .

The control strategy Eq. (15) is the same as Eq. (11), but now based on reduced state information. A reduced state vector  $\tilde{\xi}$  is guaranteed to be perpendicular to  $\tilde{\mathbf{f}}_u$  through Eq. (15), but may not lie in the plane spanned by the two unstable eigenvectors. In this case other choices for  $\tilde{\mathbf{K}}$  than that of Eq. (15) may offer better control performance, i.e., smaller

$|\lambda_c|$ . We have found this to be the case. However, the design of these vectors can only be done if the full state information about  $\mathbf{A}$  and  $\mathbf{g}$  is available.

In the case that not all modes can be registered directly in the experiment, it is possible to reconstruct the full state space from a partial measurement through embedding. In control engineering the ‘‘observer’’ technique is related to embedding, but it has a narrower scope [10]. If information about the eigenvalue associated with the  $\dot{\alpha}$  mode is hard to come by in a direct measurement, it will also be elusive in an indirect measurement through embedding. This is illustrated almost trivially in Appendix B.

## V. ESTIMATING PHASE SPACE

If no *a priori* information exists about the dynamical system, it is necessary to find in an experiment the location of unstable periodic points and their local linear neighborhood from long chaotic time series. The linear dynamics  $\xi_{n+1} - \phi_p = \mathbf{A}(\xi_n - \phi_p)$  in a small neighborhood of the unstable periodic orbit  $\phi_p$  is then estimated from the evolution of close points using a least-squares method. For the perturbed pendulum, the matrix  $\mathbf{A}$  has three very different eigenvalues, that is, the matrix  $\mathbf{A}$  is near singular. For example, for the stabilized fixed point at  $K_p=0.2$ ,  $\lambda_1=-2.0096$ ,  $\lambda_2=-0.2896$ , and  $\lambda_3=0.1449$ , with a ratio of largest to smallest eigenvalue of 14. At  $K_p=0.59$  [where the reduced control matrix Eq. (14) just becomes stable] this ratio has increased to 790 as now  $\lambda_1=-1.7334$ ,  $\lambda_2=-0.3430$ , and  $\lambda_3=0.0022$ .

Although the least-squares approach enables us to accurately pinpoint the locations of the periodic points, there are several profound problems associated with it for determining the elements of the matrix  $\mathbf{A}$ . First, the dynamics in the linear neighborhood  $\mathbf{A}$  must be found from following the evolution of phase-space points near a close return. Clearly, points that are not very close to the unstable periodic point will experience the nonlinearity of the system. The dynamics along the most stable manifolds is then overwhelmed by the local curvature of the unstable manifold. Determining small eigenvalues, therefore, requires close returns and thus long time series. Second, if the registered time series is affected by noise, the least-squares fit of  $\mathbf{A}$  to the neighborhood of  $\phi_p$  is an ill-conditioned problem, even in the absence of curvature, and the smallest eigenvalue is strongly determined by the noise level.

These problems are aggravated in an essential way by the Cantor-like structure of the measure generated by the dynamical system. This structure is clearly observed in the distribution of points near the fixed point  $(\phi, \dot{\phi}, \dot{\alpha}) = (3.0041, 6.1932, 9.1545)$  in Fig. 7. We will now quantify its effect on the least-squares analysis of the local dynamics. If  $\xi_k$  is a phase-space point that nearly returns in  $p$  steps, so that it is a candidate  $p$ -cycle, we determine the local linear neighborhood from the evolution of nearby points  $\xi_i$ ,

$$y_i = \mathbf{A}x_i + \mathbf{B}$$

where  $y_i = (\xi_{i+p} - \xi_{k+p})$ , and  $x_i = (\xi_i - \xi_k)$ , and where the vector  $\mathbf{B}$  allows for the displacement of  $\xi_k$  from the true

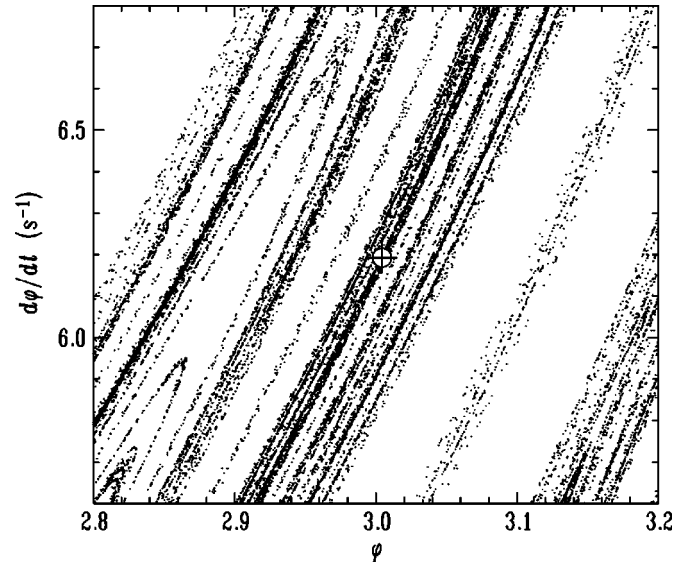


FIG. 7. Neighborhood of the unstable fixed point  $(\phi, \dot{\phi}, \dot{\alpha}) = (3.0041, 6.1932, 9.1545)$  of the perturbed pendulum at  $K_p=0.2$   $\text{kg m}^2 \text{s}^{-1}$ . The local Cantor-like structure of the attractor gives rise to logarithmic-oscillations in the scaling behavior of several quantities that are associated with control.

periodic point  $\phi_p$ . In a least-squares approach for  $N$  points in a (small) neighborhood of  $\phi_p$  the minimum of the quantity

$$\sum_{i=1}^N \|y_i - \mathbf{A}x_i - \mathbf{B}\|^2 \quad (16)$$

is sought, with the solution

$$\mathbf{A} = \mathbf{S}\mathbf{R}^{-1}. \quad (17)$$

$\mathbf{R}$  is the correlation matrix of the *support* of the least-squares fit with elements  $R_{kl} = \sum_{i=1}^N x_k^i x_l^i - (1/N) \sum_{i=1}^N x_k^i \sum_{j=1}^N x_l^j$ , and  $\mathbf{S}$  is the matrix with elements  $S_{kl} = \sum_{i=1}^N y_k^i x_l^i - (1/N) \sum_{i=1}^N y_k^i \sum_{j=1}^N x_l^j$ . On Cantor-like supports, such as shown for the pendulum in Fig. 7, the correlation matrix  $\mathbf{R}$  has a highly problematic structure. If we span a phase-space vector  $x$  by a component  $x_1$  in the expanding direction (along the bands in Fig. 7) and components  $x_2, x_3$  in the transverse contracting directions, it is readily appreciated that the  $x_{2,3}$  components are more strongly correlated than the  $x_1$  component. The result is that  $\mathbf{R}$  has very different eigenvalues. The near-singular character of the correlation matrix strongly amplifies errors, for example, errors that are due to the curvature of phase space or due to experimental noise. This error amplification property is quantified by the condition number  $C$ , which is the ratio of the largest to the smallest eigenvalue of  $\mathbf{R}$ .

From a long time series ( $10^7$  iterates), we took all  $N(r)$  iterates in balls with radius  $r$  around the unstable periodic point  $\phi_1$  shown in Fig. 7. The number of points  $N(r)$  increases with  $r$  as  $N(r) \sim r^D$  with  $D=1.61$ , which is close to the prediction of Eq. (8),  $1 + \ln|\lambda_1|/|\ln|\lambda_2||=1.56$ . The condition number  $C(r)$  was computed on these sets of points. The result is shown in Fig. 8 and should be compared to the case of completely random points, when the condition number is close to 1. As the correlation matrix  $\mathbf{R}$  is computed over

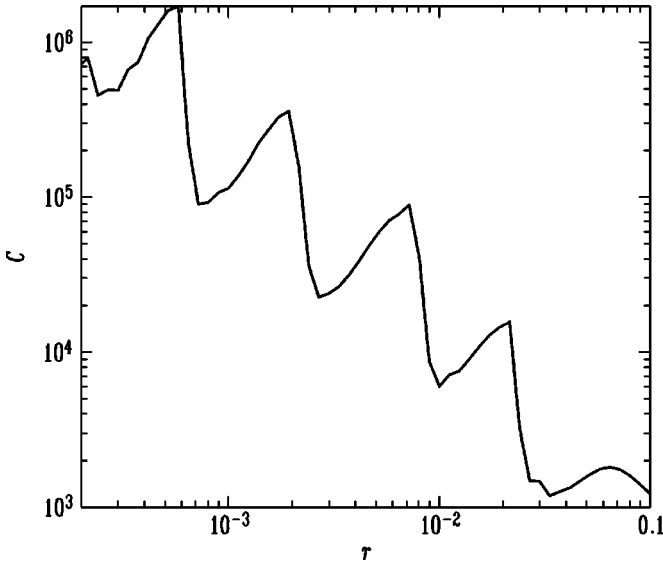


FIG. 8. Condition number of the correlation matrix  $\mathbf{R}$  as a function of the radius  $r$  of a ball around an unstable fixed point. The number of points  $N$  over which  $\mathbf{R}$  was computed increases from  $10^2$  at  $r=10^{-3}$  to  $5 \times 10^5$  at  $r=10^{-1}$ . The oscillations in  $C$  are due to the lacunarity of the measure. The radius  $r$  is normalized such that the chaotic attractor of Fig. 2 has unit extent in the  $(\phi, \dot{\phi}, \dot{\alpha})$  directions.

areas with an increasing size  $r$ , the singular character of the measure is more effectively averaged, and  $C$  decreases.

The condition number displays scaling behavior, but it is strongly modulated by regular oscillations on a logarithmic scale. The occurrence of oscillations in the scaling properties of fractal sets is very well known, and was first discussed by Mandelbrot in the context of lacunarity [17]. Lacunarity is a property of fractal sets that have holes at all scales. A well-known example is the middle-third Cantor set. Imagine a point in the Cantor set that is in the middle of an interval with length  $l$  of which we compute the measure  $\mu_l$ . When the interval reaches out to a hole,  $\mu_l$  will not change until  $l$  has grown sufficiently to reach across the gap. Because there is a geometric progression of holes in holes,  $\mu_l$  will oscillate on a logarithmic scale. Except for strictly self-similar sets, lacunarity oscillations are generically only seen in local scaling behavior, as they will not survive averaging over the chaotic attractor. In [18], precise arguments are given for survival of lacunarity oscillations in averages over multifractals.

The dramatic effect of the uneven distribution of points on an estimate of eigenvalues is illustrated in Fig. 9. The estimate was made by picking randomly 32 points  $\xi_i$  from balls with radius  $r$  around the unstable fixed point. Each of these points was iterated according to the full dynamical system Eq. (6),  $\xi'_i = \mathbf{F}(\xi_i)$ . The matrix  $\mathbf{A}$  that describes the linear evolution was then determined in a least-squares analysis [Eqs. (16) and (17)] with  $x_i = \xi_i - \phi_1$  and  $y_i = \xi'_i - \phi_1$ . The resulting eigenvalues were averaged over 32 such selections. For balls containing the natural measure, only the largest eigenvalue  $\lambda_1$  can be estimated with confidence. If the balls are, instead, filled uniformly, the error in the estimated eigenvalues is small. Let us emphasize that in both cases the nonlinearity of  $\mathbf{F}(\xi)$  is the only cause of the error; there is no

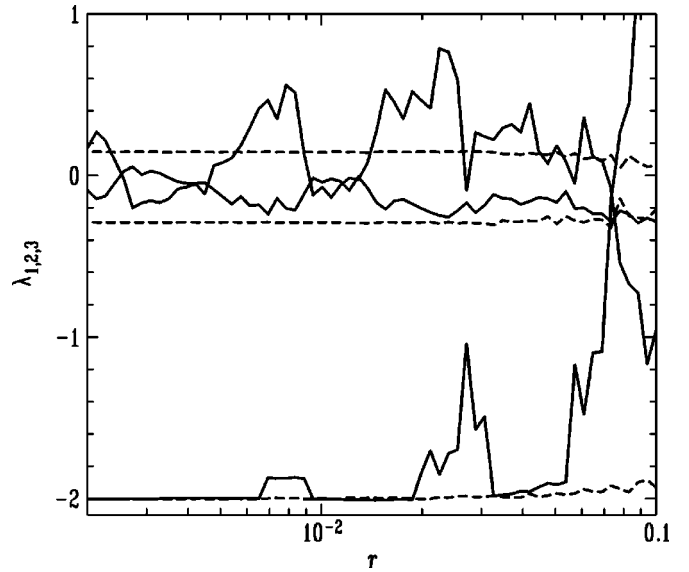


FIG. 9. Eigenvalues estimated from small neighborhoods around an unstable fixed point. The radius  $r$  is normalized such that the chaotic attractor of Fig. 2 has unit extent in the  $(\phi, \dot{\phi}, \dot{\alpha})$  directions. A least-squares analysis was done on 32 points picked randomly from spheres with radius  $r$ . The result is an average of 32 selections. Full lines: neighborhoods containing the natural measure. Dashed lines: uniformly filled neighborhoods.

noise and there is no uncertainty in the location of the fixed point. The importance of the nonlinearity depends on  $r$ , but not on the distribution of points. With an error amplification of a factor  $10^3$ , even for large neighborhoods ( $r=0.1$ ) it is nearly impossible to find the information needed for control. Clearly, it is necessary to destroy chaos in an essential manner in order to bring the condition number closer to 1.

## VI. WAITING TIME

As the oscillations in the scaling curve of Fig. 8 reflect the local Cantor structure of the measure, they will emerge in the scaling curves of all pointwise quantities. An example is the waiting time before control, for which it was predicted in Sec. III that

$$T_w \sim (q_{\max})^{(\ln|\lambda_u|/\ln|\lambda_s| - 1)/2}. \quad (18)$$

In Fig. 10 we plot the waiting time before an unstable fixed point and a period 3 orbit can be controlled. The average waiting time was computed in the unperturbed pendulum by randomly sprinkling 512 initial conditions on the phase plane, iterating each of them 256 times, and then registering the number of iterates before successful control of the unstable periodic point. For the unstable period 3 orbit we used control at each of the three cycle elements, as explained in Appendix A.

In agreement with Eq. (18), the waiting times have an algebraic dependence on the maximum allowed parameter modulation  $\Delta\Omega$ . However, the predicted dependence is only seen *on average*. In particular, the waiting time before successful control of the fixed point fluctuates wildly about its correctly predicted average dependence. These fluctuations take the form of regular oscillations in  $\log\Delta\Omega$ , such that the waiting time can be as much as a factor of 4 longer than the

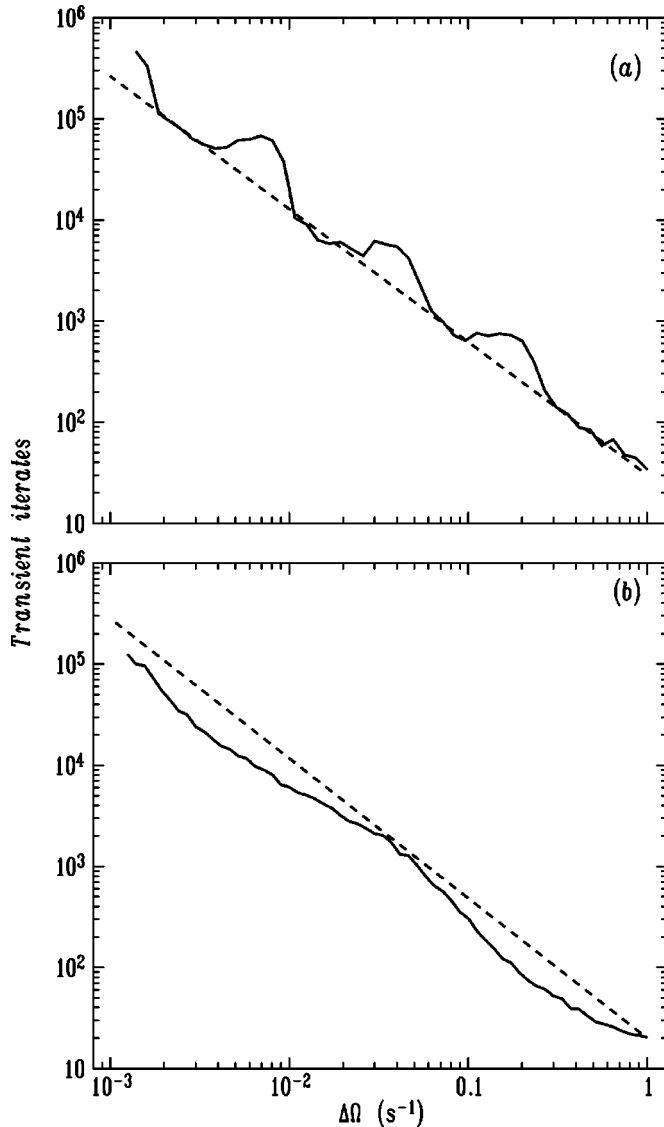


FIG. 10. (a) Average waiting time (in excitation periods) before control of a fixed point in the unperturbed pendulum as a function of the maximum allowed excursion of the driving frequency  $\Delta\Omega$ , which is used as the control parameter. For each  $\Delta\Omega$ , 512 initial points were randomly sprinkled over the square  $\phi \in [0, 2\pi]$ ,  $\dot{\phi} \in [-20, 20]$ , each of them iterated 256 times, after which the number of iterates before successful control was registered. The slope of the dashed line is the prediction of Eq.(13). (b) Same as (a), but for control of an unstable period 3 orbit.

prediction of Eq. (13). Because cycles with larger periods sample more regions of phase space, we expect that the oscillations of longer cycles are averaged more effectively.

Although the waiting time before control reflects an interesting facet of the control of chaos, it is not necessary to wait so long before control can be enacted. With crude knowledge of the dynamics it is possible to steer a wandering orbit onto the target neighborhood [16].

## VII. CONCLUSION

For the weakly perturbed pendulum the idea that control of chaos can be done on the basis of experimental information alone simply breaks down. As a weak interaction with

the environment characterized by a small eigenvalue is a generic problem, we expect that the sketched route to failure of chaos control must be a common one. For successful control we are forced to consider the dynamics of the  $\dot{\alpha}$  coordinate when it has no dynamics of its own. Unfortunately, there is not a simple transformation that eliminates the  $\dot{\alpha}$  dynamics using the information in an experimental time series. We believe that it can be done only using a faithful model of the experiment.

Our most important conclusion is the impossibility of learning the needed information due to the nonlinearity of the system and the fractal nature of chaos. It does not help to split the linear dynamics  $\mathbf{A}$  over  $N$  partial sections  $\alpha_i = i2\pi/N, i = 1, \dots, N$ , and determine the partial matrices  $\mathbf{A}_i$  for each of them. We have found that the error in  $\mathbf{A} = \mathbf{A}_1 \cdots \mathbf{A}_N$  now simply accumulates.

It may be that the necessity of including information about the small eigenvalues of  $\mathbf{A}$  is due to the control scheme used. The control strategy of [1] and its variants act on the system at discrete times. In our case this is at each cycle of the excitation. Perhaps it is possible to act  $N$  times at  $\alpha_i = i2\pi/N, i = 1, \dots, N$ , and use the (still inaccurate) matrices  $\mathbf{A}_i$  such that the resulting control action is stable.

Better estimates of the local linear neighborhood of unstable periodic points with near-singular Jacobian  $\mathbf{A}$  may be obtained by estimating the elements of  $\mathbf{A}$  using random modulations of the control parameter. This should result in a more even distribution of points in small neighborhoods of unstable periodic orbits than is given by the natural measure. The location of unstable periodic points may then first be learned from a time series, after which noise is fed to the system in order to determine the evolution of their linear neighborhoods.

## ACKNOWLEDGMENTS

We gratefully acknowledge financial support by the Nederlandse Organisatie voor Wetenschappelijk Onderzoek (NWO). We also thank Henk Nijmeijer and Thomas Schreiber for enlightening discussions.

## APPENDIX A: CONTROLLING PERIOD- $p$ UNSTABLE ORBITS

We will describe the extension of the control method to the stabilization of unstable period- $p$  cycles. Another application of this extension is to take control  $N$  times (at  $\alpha_i = i2\pi/N, i = 1, \dots, N$ ) in each excitation cycle, in order to overcome problems with rapid expansion near very unstable periodic points.

A period- $p$  cycle consists of  $p$  cycle elements  $\phi_p^{(1)}, \dots, \phi_p^{(p)}$  in the Poincaré section. The control strategy is to steer the orbit onto the stable eigenvector  $e_s^{(i)}$  of the nearest cycle element  $\phi_p^{(i)}$  at each Poincaré intersection. Without loss of generality we will describe the principle in two dimensions with one unstable  $e_u$  and one stable  $e_s$  eigenvector.

The linear neighborhood of the point  $\phi_p^{(1)}$  is mapped onto that of cycle element  $\phi_p^{(2)}$  by the partial matrix  $\mathbf{A}_1$ , much as the partial matrix  $\mathbf{A}_i$  relates the linear neighborhoods of the

cycle elements  $\phi_p^{(i)}$  and  $\phi_p^{(i+1)}$ . The neighborhood of  $\phi_p^{(1)}$  will be mapped onto itself after a complete cycle of  $p$  Poincaré sections by the composed matrix  $\mathbf{A}^{(1)} = \mathbf{A}_p \mathbf{A}_{p-1} \cdots \mathbf{A}_1$ . In the same manner the neighborhood of  $\phi_p^{(i)}$  will be mapped onto itself by the matrix  $\mathbf{A}^{(i)} = \mathbf{A}_{p-i+1} \cdots \mathbf{A}_1 \mathbf{A}_p \cdots \mathbf{A}_{i+1} \mathbf{A}_i$ .

The eigenvectors of the cycle element  $\phi_p^{(i)}$  then follow from

$$\mathbf{A}^{(i)} \mathbf{e}_{u,s}^{(i)} = \lambda_{u,s}^{(i)} \mathbf{e}_{u,s}^{(i)}. \quad (\text{A1})$$

Controlling period- $p$  orbits should be done by adjusting the control parameter at each of the  $p$  Poincaré intersections, as the complete cycles have very large eigenvalues.

The eigenvectors  $\mathbf{e}_{u,s}^{(1)}, \dots, \mathbf{e}_{u,s}^{(p)}$  are related in the following way:

$$\mathbf{A}_i \mathbf{e}_{u,s}^{(i)} = \lambda_{u,s}^{(i+1)} \mathbf{e}_{u,s}^{(i+1)} \quad \text{with} \quad \lambda_{u,s}^{(i+1)} = \mathbf{e}_{u,s}^{(i+1)} \cdot \mathbf{A}_i \mathbf{e}_{u,s}^{(i)}. \quad (\text{A2})$$

To facilitate the implementation of the control strategy Eq. (11), the matrix  $\mathbf{A}_i$  can be written in covariant notation,

$$\mathbf{A}_i = [\lambda_u^{(i+1)} \mathbf{e}_u^{(i+1)} \mathbf{f}_u^{(i)} + \lambda_s^{(i+1)} \mathbf{e}_s^{(i+1)} \mathbf{f}_s^{(i)}], \quad (\text{A3})$$

where the vectors  $\mathbf{f}_{u,s}^{(i)}$  are defined as before:  $\mathbf{f}_u^{(i)} \cdot \mathbf{e}_u^{(i)} = 1$ ,  $\mathbf{f}_u^{(i)} \cdot \mathbf{e}_s^{(i)} = 0$ ,  $\mathbf{f}_s^{(i)} \cdot \mathbf{e}_u^{(i)} = 0$ , and  $\mathbf{f}_s^{(i)} \cdot \mathbf{e}_s^{(i)} = 1$ . The dynamics between subsequent Poincaré sections then is

$$\begin{aligned} \xi_{i+1} - q_i \mathbf{g}^{(i+1)} &= [\lambda_u^{(i+1)} \mathbf{e}_u^{(i+1)} \mathbf{f}_u^{(i)} \\ &+ \lambda_s^{(i+1)} \mathbf{e}_s^{(i+1)} \mathbf{f}_s^{(i)}] (\xi_i - q_i \mathbf{g}^{(i)}), \end{aligned} \quad (\text{A4})$$

where  $\mathbf{g}^{(i)}$  is the sensitivity to parameter variations of the cycle element  $\phi_p^{(i)}$ . The control strategy now is the requirement that  $\xi_{i+1}$  is on the stable eigenvector  $\mathbf{e}_s^{(i+1)}$ ,

$$q_i = \frac{\lambda_u^{(i+1)} (\mathbf{f}_u^{(i)} \cdot \xi_i)}{\lambda_u^{(i+1)} (\mathbf{f}_u^{(i)} \cdot \mathbf{g}^{(i)}) - (\mathbf{f}_u^{(i+1)} \cdot \mathbf{g}^{(i+1)})}. \quad (\text{A5})$$

We have used this form for controlling unstable period- $p$  orbits of the pendulum.

We note emphatically that the  $\lambda_{u,s}^{(i)}$  are *not* the eigenvalues of the partial matrices  $\mathbf{A}_i$ . In [5,6] a control strategy based on these eigenvalues is described. As is evident from [5], such a strategy is extremely problematic because the eigenvalues of  $\mathbf{A}_i$  may be complex.

## APPENDIX B: EMBEDDING

Embedding amounts to usage of the time history of the system in order to reconstruct its full state space. In fact, this has become a customary procedure in control attempts of systems whose instantaneous location in state space cannot be characterized completely. The key idea is that a  $D$ -dimensional state space can be reconstructed from a time series of measurements  $\xi(i\tau)$  of a single component  $\xi(t)$  using delay coordinates  $\hat{\xi} = (\xi(i\tau), \xi((i+1)\tau), \dots, \xi((i$

$+2D+1)\tau)$ . The resulting state space has under certain conditions a one-to-one relation with the true state space [2].

The goal is to construct the full phase space from  $(\phi_n, \dot{\phi}_n)$  measurements using the delay coordinates  $(\phi_n, \dot{\phi}_n)$ , and  $(\phi_{n+1}, \dot{\phi}_{n+1})$ . It is instructive to write out the dynamics of the perturbed pendulum in an embedded state space. At Poincaré section  $n$  the delay vectors  $\hat{\xi}_n$  are

$$\hat{\xi}_n = \begin{pmatrix} \tilde{\xi}_{n+1} \\ \tilde{\xi}_n \end{pmatrix}. \quad (\text{B1})$$

The evolution of the embedded state vector  $\hat{\xi}_n$  can be seen by augmenting the truncated vectors  $\tilde{\xi}$  back to the full system,

$$\begin{pmatrix} \tilde{\xi}_{n+1} \\ \dot{\alpha}_{n+1} \end{pmatrix} = \begin{pmatrix} \tilde{\mathbf{A}} & \mathbf{B}^T \\ \mathbf{B} & a \end{pmatrix} \begin{pmatrix} \tilde{\xi}_n \\ \dot{\alpha}_n \end{pmatrix} + p_n \begin{pmatrix} \tilde{\mathbf{u}} \\ u_3 \end{pmatrix}, \quad (\text{B2})$$

where the row vector  $\mathbf{B}$  consists of the two row elements that were deleted from the Jacobian  $\mathbf{A}$  in order to reduce it to two dimensions, and similarly for the column vector  $\mathbf{B}^T$ . Equation (B2) can be iterated to eliminate the dependence on the angular frequency  $\dot{\alpha}$  of the drive. The result is a complete description of the full state space in terms of  $\tilde{\xi}$ , but at the expense of time history,

$$\begin{aligned} \tilde{\xi}_{n+1} &= (\tilde{\mathbf{A}} + a\mathbf{I}) \tilde{\xi}_n + (\mathbf{B}^T \mathbf{B} - a\tilde{\mathbf{A}}) \tilde{\xi}_{n-1} \\ &+ \tilde{\mathbf{u}} p_n + (\mathbf{B}^T u_3 - a\tilde{\mathbf{u}}) p_{n-1}, \end{aligned} \quad (\text{B3})$$

which is equivalent to the evolution of the embedded system

$$\begin{aligned} \hat{\xi}_{n+1} &= \begin{pmatrix} \tilde{\mathbf{A}} + a\mathbf{I} & \mathbf{B}^T \mathbf{B} - a\tilde{\mathbf{A}} \\ \mathbf{I} & 0 \end{pmatrix} \hat{\xi}_n + p_n \begin{pmatrix} \tilde{\mathbf{u}} \\ 0 \end{pmatrix} \\ &+ p_{n-1} \begin{pmatrix} \mathbf{B}^T u_3 - a\tilde{\mathbf{u}} \\ 0 \end{pmatrix}. \end{aligned} \quad (\text{B4})$$

Because the embedded system Eq. (B4) involves the past history  $p_{n-1}$  of the system parameter, the control strategy is more complicated than Eq. (11) for fixed points or Eq. (A5) for longer periodicities. These complications were first noticed by Dressler and Nitsche [19]. Embedding, therefore, has a price. We believe that embedding is not unavoidable in experiments. With modern computerized instrumentation, complete information about a system's state space should be obtained readily.

The problem that the small eigenvalue (and associated eigenvectors) of the  $\dot{\alpha}$  dynamics is very difficult to find from time series is not cured by embedding. The small eigenvalue is now reflected in the small value of  $\|\mathbf{B}^T \mathbf{B} - a\tilde{\mathbf{A}}\|$  and  $\|\mathbf{B}^T u_3 - a\tilde{\mathbf{u}}\|$  which determine the dependence of  $\tilde{\xi}_{n+1}$  on past history  $\tilde{\xi}_{n-1}$  and  $p_{n-1}$ . As this information is now needed to devise a control scheme, nothing is gained by embedding.

- [1] E. Ott, C. Grebogi, and J.A. Yorke, Phys. Rev. Lett. **64**, 1196 (1990).
- [2] T. Sauer, J.A. Yorke, and M. Casdagli, J. Stat. Phys. **65**, 579 (1991).
- [3] W. van de Water, M. Hoppenbrouwers, and F. Christiansen, Phys. Rev. A **44**, 6388 (1991).
- [4] W.L. Ditto, S.N. Rauseo, and M.L. Spano, Phys. Rev. Lett. **65**, 3211 (1991); R.J. de Korte, J.C. Schouten, and C.M. van den Bleek, Phys. Rev. E **52**, 3358 (1995).
- [5] B. Hübinger, R. Doerner, W. Martienssen, M. Herdering, R. Pitka, and U. Dressler, Phys. Rev. E **50**, 932 (1994); B. Hübinger, R. Doerner, W. Martienssen, Z. Phys. B: Condens. Matter **90**, 103 (1993).
- [6] D.J. Christini, J.J. Collins, and P.S. Lindsay, Phys. Rev. E **54**, 4824 (1996).
- [7] V. In, W.L. Ditto, M. Ding, W. Yang, M.L. Spano, and B.J. Gluckman, Phys. Rev. E **55**, 4935 (1997).
- [8] E.J. Kostelich, Physica D **58**, 138 (1992).
- [9] B.I. Epureanu and E.H. Dowell, Phys. Rev. E **56**, 5327 (1997).
- [10] K. Ogata, *Modern Control Engineering* (Prentice-Hall, London, 1990).
- [11] J.L. Kaplan and J.A. Yorke, in *Functional Differential Equations and Approximation of Fixed Points*, Vol. 730 of *Lecture Series in Mathematics*, edited by H.O. Peitgen and H.O. Walthier (Springer, Berlin, 1979), p. 204.
- [12] J. Theiler, Phys. Rev. A **36**, 4456 (1987).
- [13] D.J. Acheson and T. Mullin, Nature (London) **366**, 215 (1993). In a companion paper [D.J. Acheson, Proc. R. Soc. London, Ser. A **443**, 239 (1993)] a theorem is formulated for the stability of multiple stacked inverted pendulums whose support is vertically oscillated.
- [14] C. Grebogi, Physica D **58**, 165 (1992).
- [15] A noteworthy attempt to deduce unstable periodic points in a parametric pendulum from an approximate symbolic dynamics was reported by S.R. Bishop, D.L. Xu, and M.J. Clifford, Proc. R. Soc. London, Ser. A **452**, 1789 (1996).
- [16] T. Shinbrot, E. Ott, C. Grebogi, and J.A. Yorke, Phys. Rev. Lett. **65**, 3215 (1990); T. Shinbrot, W. Ditto, C. Grebogi, E. Ott, M. Spano, and J.A. Yorke, *ibid.* **68**, 2863 (1992).
- [17] B. Mandelbrot, *The Fractal Geometry of Nature* (Freeman & Co, San Francisco, 1982).
- [18] W. van de Water and P.P.J.M. Schram, Phys. Lett. A **140A**, 173 (1989).
- [19] U. Dressler and G. Nitsche, Phys. Rev. Lett. **68**, 1 (1991).